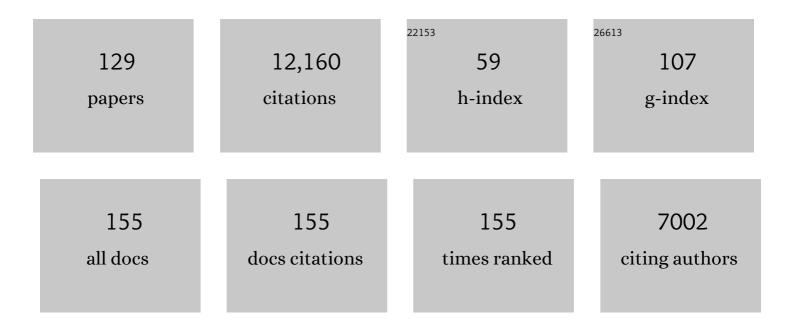
Craig E Manning

List of Publications by Year in descending order

Source: https://exaly.com/author-pdf/3096009/publications.pdf Version: 2024-02-01



#	Article	IF	CITATIONS
1	The chemistry of subduction-zone fluids. Earth and Planetary Science Letters, 2004, 223, 1-16.	4.4	682
2	Permeability of the continental crust: Implications of geothermal data and metamorphic systems. Reviews of Geophysics, 1999, 37, 127-150.	23.0	553
3	Reevaluating carbon fluxes in subduction zones, what goes down, mostly comes up. Proceedings of the United States of America, 2015, 112, E3997-4006.	7.1	492
4	The solubility of quartz in H2O in the lower crust and upper mantle. Geochimica Et Cosmochimica Acta, 1994, 58, 4831-4839.	3.9	480
5	Tectonic evolution of the early Mesozoic blueschist-bearing Qiangtang metamorphic belt, central Tibet. Tectonics, 2003, 22, n/a-n/a.	2.8	351
6	Blueschist-bearing metamorphic core complexes in the Qiangtang block reveal deep crustal structure of northern Tibet. Geology, 2000, 28, 19.	4.4	306
7	Geochronologic and thermobarometric constraints on the evolution of the Main Central Thrust, central Nepal Himalaya. Journal of Geophysical Research, 2001, 106, 16177-16204.	3.3	281
8	Low heat flow inferred from >4 Gyr zircons suggests Hadean plate boundary interactions. Nature, 2008, 456, 493-496.	27.8	259
9	The global range of subduction zone thermal structures from exhumed blueschists and eclogites: Rocks are hotter than models. Earth and Planetary Science Letters, 2015, 428, 243-254.	4.4	258
10	Subducting carbon. Nature, 2019, 574, 343-352.	27.8	250
11	Quartz solubility in H2O-NaCl and H2O-CO2 solutions at deep crust-upper mantle pressures and temperatures: 2–15 kbar and 500–900°C. Geochimica Et Cosmochimica Acta, 2000, 64, 2993-3005.	3.9	236
12	Tectonic evolution of the northeastern Pamir: Constraints from the northern portion of the Cenozoic Kongur Shan extensional system, western China. Bulletin of the Geological Society of America, 2004, 116, 953.	3.3	219
13	Geological implications of a permeability-depth curve for the continental crust. Geology, 1999, 27, 1107.	4.4	213
14	Emerging geothermometers for estimating slab surface temperatures. Nature Geoscience, 2009, 2, 611-615.	12.9	195
15	Cenozoic evolution of the eastern Pamir: Implications for strain-accommodation mechanisms at the western end of the Himalayan-Tibetan orogen. Bulletin of the Geological Society of America, 2007, 119, 882-896.	3.3	187
16	Late Paleozoic tectonic history of the Ertix Fault in the Chinese Altai and its implications for the development of the Central Asian Orogenic System. Bulletin of the Geological Society of America, 2007, 119, 944-960.	3.3	186
17	Structural evolution of the Gurla Mandhata detachment system, southwest Tibet: Implications for the eastward extent of the Karakoram fault system. Bulletin of the Geological Society of America, 2002, 114, 428-447.	3.3	182
18	Records of the evolution of the Himalayan orogen from in situ Th–Pb ion microprobe dating of monazite: Eastern Nepal and western Garhwal. Journal of Asian Earth Sciences, 2002, 20, 459-479.	2.3	181

#	Article	IF	CITATIONS
19	Early Paleozoic Tectonic and Thermomechanical Evolution of Ultrahigh-Pressure (UHP) Metamorphic Rocks in the Northern Tibetan Plateau, Northwest China. International Geology Review, 2007, 49, 681-716.	2.1	179
20	Rutile solubility in H2O, H2O–SiO2, and H2O–NaAlSi3O8 fluids at 0.7–2.0ÂGPa and 700–1000°C: Implications for mobility of nominally insoluble elements. Chemical Geology, 2008, 255, 283-293.	3.3	176
21	Permeability of the continental crust: dynamic variations inferred from seismicity and metamorphism. Geofluids, 2010, 10, 193-205.	0.7	176
22	Title is missing!. , 2011, 7, 1013.		176
23	High-temperature equilibrium isotope fractionation of non-traditional stable isotopes: Experiments, theory, and applications. Chemical Geology, 2015, 395, 176-195.	3.3	163
24	The solubility of calcite in water at 6?16ïį½kbar and 500?800ïį½ïį½C. Contributions To Mineralogy and Petrology, 2003, 146, 275-285.	3.1	152
25	Equilibrium high-temperature Fe isotope fractionation between fayalite and magnetite: An experimental calibration. Earth and Planetary Science Letters, 2008, 268, 330-338.	4.4	145
26	Spinel–olivine magnesium isotope thermometry in the mantle and implications for the Mg isotopic composition of Earth. Earth and Planetary Science Letters, 2009, 288, 524-533.	4.4	142
27	Constraints on Hadean geodynamics from mineral inclusions in >4Ga zircons. Earth and Planetary Science Letters, 2010, 298, 367-376.	4.4	141
28	Significant late Neogene east-west extension in northern Tibet. Geology, 1999, 27, 787.	4.4	137
29	Experimental determination of calcite solubility in H ₂ O-NaCl solutions at deep crust/upper mantle pressures and temperatures: Implications for metasomatic processes in shear zones. American Mineralogist, 2002, 87, 1401-1409.	1.9	128
30	Ultralow viscosity of carbonate melts at high pressures. Nature Communications, 2014, 5, 5091.	12.8	124
31	Global variations in H ₂ O/Ce: 1. Slab surface temperatures beneath volcanic arcs. Geochemistry, Geophysics, Geosystems, 2012, 13, .	2.5	122
32	Solubility of CePO4 monazite and YPO4 xenotime in H2O and H2O–NaCl at 800°C and 1GPa: Implications for REE and Y transport during high-grade metamorphism. Chemical Geology, 2011, 282, 58-66.	3.3	118
33	The Chemistry of Carbon in Aqueous Fluids at Crustal and Upper-Mantle Conditions: Experimental and Theoretical Constraints. Reviews in Mineralogy and Geochemistry, 2013, 75, 109-148.	4.8	115
34	Very low solubility of rutile in H2O at high pressure and temperature, and its implications for Ti mobility in subduction zones. American Mineralogist, 2005, 90, 502-505.	1.9	113
35	Rutile solubility in albite-H2O and Na2Si3O7-H2O at high temperatures and pressures by in-situ synchrotron radiation micro-XRF. Earth and Planetary Science Letters, 2008, 272, 730-737.	4.4	111
36	Zircon solubility and zirconium complexation in H2O+Na2O+SiO2±Al2O3 fluids at high pressure and temperature. Earth and Planetary Science Letters, 2012, 349-350, 15-25.	4.4	108

#	Article	IF	CITATIONS
37	Formation of methane on Mars by fluid-rock interaction in the crust. Geophysical Research Letters, 2005, 32, .	4.0	107
38	Thermodynamics of SiO2–H2O fluid near the upper critical end point from quartz solubility measurements at 10Âkbar. Earth and Planetary Science Letters, 2008, 274, 241-249.	4.4	97
39	Fluids of the Lower Crust: Deep Is Different. Annual Review of Earth and Planetary Sciences, 2018, 46, 67-97.	11.0	96
40	Solubility of enstatite + forsterite in H2O at deep crust/upper mantle conditions: 4 to 15 kbar and 700 to 900°c. Geochimica Et Cosmochimica Acta, 2002, 66, 4165-4176.	3.9	95
41	Implications for metal and volatile cycles from the pH of subduction zone fluids. Nature, 2016, 539, 420-424.	27.8	93
42	Rapid high-temperature metamorphism of East Pacific Rise gabbros from Hess Deep. Earth and Planetary Science Letters, 1996, 144, 123-132.	4.4	88
43	Brine-assisted anatexis: Experimental melting in the system haplogranite–H2O–NaCl–KCl at deep-crustal conditions. Earth and Planetary Science Letters, 2013, 374, 111-120.	4.4	87
44	Geology, Age and Origin of Supracrustal Rocks at Akilia, West Greenland. Numerische Mathematik, 2006, 306, 303-366.	1.4	81
45	Solubility of corundum + kyanite in H2O at 700°C and 10 kbar: evidence for Al-Si complexing at high pressure and temperature. Geofluids, 2007, 7, 258-269.	0.7	77
46	Metamorphic evolution, mineral chemistry and thermobarometry of orthogneiss hosting ultrahigh-pressure eclogites in the North Qaidam metamorphic belt, Western China. Journal of Asian Earth Sciences, 2009, 35, 273-284.	2.3	77
47	Fluorapatite solubility in H2O and H2O–NaCl at 700 to 900°C and 0.7 to 2.0ÂGPa. Chemical Geology, 2008, 251, 112-119.	3.3	76
48	Brines at high pressure and temperature: Thermodynamic, petrologic and geochemical effects. Precambrian Research, 2014, 253, 6-16.	2.7	76
49	Solubilities of corundum, wollastonite and quartz in H2O–NaCl solutions at 800°C and 10kbar: Interaction of simple minerals with brines at high pressure and temperature. Geochimica Et Cosmochimica Acta, 2006, 70, 5571-5582.	3.9	74
50	Tectonic development of the southern Chinese Altai Range as determined by structural geology, thermobarometry, ⁴⁰ Ar/ ³⁹ Ar thermochronology, and Th/Pb ion-microprobe monazite geochronology. Bulletin of the Geological Society of America, 2009, 121, 1381-1393.	3.3	74
51	Rutile solubility in supercritical NaAlSi3O8–H2O fluids. Chemical Geology, 2011, 284, 74-81.	3.3	74
52	Premelting polymerization of crustal and mantle fluids, as indicated by the solubility of albite+paragonite+quartz in H2O at 1GPa and 350–620°C. Earth and Planetary Science Letters, 2010, 292, 325-336.	4.4	73
53	Dehydration melting and the relationship between granites and granulites. Precambrian Research, 2014, 253, 26-37.	2.7	72
54	Activity coefficient and polymerization of aqueous silica at 800��C, 12�kbar, from solubility measurements on SiO2-buffering mineral assemblages. Contributions To Mineralogy and Petrology, 2003, 146, 135-143.	3.1	71

7.1

48

#	ARTICLE Experimental determination of <scp><scp>CePO</scp>₄</scp> and	IF	CITATIONS
55	<pre><scp><scp>YPO</scp>₄</scp> solubilities in <scp><scp>H₂O</scp></scp>alt a00Ű<scp>C</scp> and 1ÅGPa: implications for rare earth element transport in highâ€grade metamorphic fluids. Geofluids, 2013, 13, 272 2020</pre>	0.7	69
56	The solubility of corundum in H2O at high pressure and temperature and its implications for Al mobility in the deep crust and upper mantle. Chemical Geology, 2007, 240, 54-60.	3.3	68
57	The solubility of rocks in metamorphic fluids: A model for rock-dominated conditions to upper mantle pressure and temperature. Earth and Planetary Science Letters, 2015, 430, 486-498.	4.4	68
58	A short timescale for changing oxygen fugacity in the solar nebula revealed by high-resolution 26Al–26Mg dating of CAI rims. Earth and Planetary Science Letters, 2005, 238, 272-283.	4.4	66
59	Thermodynamic model for mineral solubility in aqueous fluids: theory, calibration and application to model fluidâ€flow systems. Geofluids, 2010, 10, 20-40.	0.7	65
60	The Substitution of Al and F in Titanite at High Pressure and Temperature: Experimental Constraints on Phase Relations and Solid Solution Properties. Journal of Petrology, 2002, 43, 1787-1814.	2.8	63
61	Solubility of corundum in the system Al2O3–SiO2–H2O–NaCl at 800°C and 10Âkbar. Chemical Geology, 2008, 249, 250-261.	3.3	62
62	Polymerization of aqueous silica in H2O–K2O solutions at 25–200°C and 1bar to 20kbar. Chemical Geology, 2011, 283, 161-170.	3.3	59
63	The solubility of fluorite in H2O and H2O–NaCl at high pressure and temperature. Chemical Geology, 2007, 242, 299-306.	3.3	58
64	Thermodynamic Modeling of Fluid-Rock Interaction at Mid-Crustal to Upper-Mantle Conditions. Reviews in Mineralogy and Geochemistry, 2013, 76, 135-164.	4.8	57
65	Crystal chemical constraints on inter-mineral Fe isotope fractionation and implications for Fe isotope disequilibrium in San Carlos mantle xenoliths. Geochimica Et Cosmochimica Acta, 2015, 154, 168-185.	3.9	57
66	Abiogenic methanogenesis during experimental komatiite serpentinization: Implications for the evolution of the early Precambrian atmosphere. Chemical Geology, 2012, 326-327, 102-112.	3.3	54
67	Phase-Equilibrium Controls on SiO ₂ Metasomatism by Aqueous Fluid in Subduction Zones: Reaction at Constant Pressure and Temperature. International Geology Review, 1995, 37, 1074-1093.	2.1	53
68	Role of saline fluids in deepâ€crustal and upperâ€mantle metasomatism: insights from experimental studies. Geofluids, 2010, 10, 58-72.	0.7	53
69	Is Mars alive?. Eos, 2006, 87, 433.	0.1	50
70	A thermodynamic model for the system <mml:math <br="" xmlns:mml="http://www.w3.org/1998/Math/MathML">altimg="si32.gif" overflow="scroll"><mml:mrow><mml:mrow><mml:mrow><mml:mtext>SiO</mml:mtext></mml:mrow><mml:mro near the upper critical end point based on quartz solubility experiments at 500â€"1100 °C and 5â€"2.</mml:mro </mml:mrow></mml:mrow></mml:math>	vøxy mml:	m #n ≫2
71	Geochimica Et Cosmochimica Acta, 2012, 86, 196-213. Experimental determination of equilibrium magnesium isotope fractionation between spinel, forsterite, and magnesite from 600 to 800 ŰC. Geochimica Et Cosmochimica Acta, 2013, 118, 18-32.	3.9	49

⁷² Diffuse fluid flux through orogenic belts: Implications for the world ocean. Proceedings of the National Academy of Sciences of the United States of America, 2002, 99, 9113-9116.

#	Article	IF	CITATIONS
73	Dolomite III: A new candidate lower mantle carbonate. Geophysical Research Letters, 2011, 38, n/a-n/a.	4.0	48
74	Hydrothermal clinopyroxenes of the Skaergaard intrusion. Contributions To Mineralogy and Petrology, 1986, 92, 437-447.	3.1	47
75	Absence of amorphous forms when ice is compressed at low temperature. Nature, 2019, 569, 542-545.	27.8	47
76	Fractal clustering of metamorphic veins. Geology, 1994, 22, 335-338.	4.4	46
77	Experimental investigation of the solubility of albite and jadeite in H2O, with paragonite+quartz at 500 and 600°C, and 1–2.25GPa. Geochimica Et Cosmochimica Acta, 2011, 75, 2924-2939.	3.9	46
78	Phaseâ€equilibrium constraints on titanite and rutile activities in mafic epidote amphibolites and geobarometry using titanite–rutile equilibria. Journal of Metamorphic Geology, 2009, 27, 509-521.	3.4	45
79	Experimental determination of equilibrium nickel isotope fractionation between metal and silicate from 500°C to 950°C. Geochimica Et Cosmochimica Acta, 2012, 86, 276-295.	3.9	45
80	Subduction-Zone Fluids. Elements, 2020, 16, 395-400.	0.5	45
81	Mobilizing aluminum in crustal and mantle fluids. Journal of Geochemical Exploration, 2006, 89, 251-253.	3.2	41
82	Solubility of grossular, Ca3Al2Si3O12, in H2O–NaCl solutions at 800°C and 10kbar, and the stability of garnet in the system CaSiO3–Al2O3–H2O–NaCl. Geochimica Et Cosmochimica Acta, 2007, 71, 5191-5202.	. 3.9	40
83	The Behavior of Halogens During Subduction-Zone Processes. Springer Geochemistry, 2018, , 545-590.	0.1	39
84	Hydration state and activity of aqueous silica in H2O-CO2 fluids at high pressure and temperature. American Mineralogist, 2009, 94, 1287-1290.	1.9	38
85	A piece of the deep carbon puzzle. Nature Geoscience, 2014, 7, 333-334.	12.9	38
86	Layering in the wall rock of Valles Marineris: intrusive and extrusive magmatism. Geophysical Research Letters, 2003, 30, .	4.0	34
87	Detection of liquid H ₂ O in vapor bubbles in reheated melt inclusions: Implications for magmatic fluid composition and volatile budgets of magmas?. American Mineralogist, 2016, 101, 1691-1695.	1.9	32
88	The current status of titanite–rutile thermobarometry in ultrahigh-pressure metamorphic rocks: The influence of titanite activity models on phase equilibrium calculations. Chemical Geology, 2008, 254, 123-132.	3.3	31
89	Argon, oxygen, and boron isotopic evidence documenting 40ArE accumulation in phengite during water-rich high-pressure subduction metasomatism of continental crust. Earth and Planetary Science Letters, 2016, 446, 56-67.	4.4	30
90	High-pressure compressibility and thermal expansion of aragonite. American Mineralogist, 2016, 101, 1651-1658.	1.9	30

#	Article	IF	CITATIONS
91	Experimental determination of the viscosity of Na2CO3 melt between 1.7 and 4.6â€GPa at 1200–1700â€~°C: Implications for the rheology of carbonatite magmas in the Earth's upper mantle. Chemical Geology, 2018, 501, 19-25.	3.3	29
92	Experimental determination of quartz solubility and melting in the system SiO2–H2O–NaCl at 15–20Âkbar and 900–1100°C: implications for silica polymerization and the formation of supercritical fluids. Contributions To Mineralogy and Petrology, 2015, 170, 1.	3.1	27
93	Carbon sequestration during core formation implied by complex carbon polymerization. Nature Communications, 2019, 10, 789.	12.8	27
94	Gibbs Free Energy of Formation of Zircon from Measurement of Solubility in H2O. Journal of the American Ceramic Society, 2005, 88, 1854-1858.	3.8	24
95	Coupled Reaction and Flow in Subduction Zones: Silica Metasomatism in the Mantle Wedge. , 1997, , 139-148.		24
96	Experimental determination of the equilibria: rutile + magnesite = geikielite + CO2and zircon + 2 magnesite = baddeleyite + forsterite + 2 CO2. American Mineralogist, 2002, 87, 1342-1350.	1.9	22
97	Solubility of andradite, Ca3Fe2Si3O12, in a 10 mol% NaCl solution at 800 ÂC and 10 kbar: Implications for the metasomatic origin of grandite garnet in calc-silicate granulites. American Mineralogist, 2008, 93, 886-892.	1.9	22
98	Solubility of corundum in aqueous KOH solutions at 700°C and 1ÂGPa. Chemical Geology, 2009, 262, 310-317.	3.3	22
99	Diopside, enstatite and forsterite solubilities in H2O and H2O-NaCl solutions at lower crustal and upper mantle conditions. Geochimica Et Cosmochimica Acta, 2020, 279, 119-142.	3.9	21
100	Aluminum speciation in aqueous fluids at deep crustal pressure and temperature. Geochimica Et Cosmochimica Acta, 2014, 133, 128-141.	3.9	20
101	An experimental study of OH solubility in rutile at 500-900 ÂC, 0.5-2 GPa, and a range of oxygen fugacities. American Mineralogist, 2011, 96, 1291-1299.	1.9	19
102	Dissolution susceptibility of glass-like carbon versus crystalline graphite in high-pressure aqueous fluids and implications for the behavior of organic matter in subduction zones. Geochimica Et Cosmochimica Acta, 2020, 273, 383-402.	3.9	19
103	Free energy of formation of zircon based on solubility measurements at high temperature and pressure. American Mineralogist, 2010, 95, 52-58.	1.9	18
104	Redox effects on calcite-portlandite-fluid equilibria at forearc conditions: Carbon mobility, methanogenesis, and reduction melting of calcite. American Mineralogist, 2014, 99, 1604-1615.	1.9	18
105	Implications of crustal permeability for fluid movementbetween terrestrial fluid reservoirs. Journal of Geochemical Exploration, 2003, 78-79, 1-6.	3.2	17
106	The solubility of apatite in H2O, KCl-H2O, NaCl-H2O at 800 °C and 1.0 GPa: Implications for REE mobility in high-grade saline brines. Chemical Geology, 2017, 470, 180-192.	3.3	17
107	Brittle Deformation of Carbonated Peridotite—Insights From Listvenites of the Samail Ophiolite (Oman Drilling Project Hole BT1B). Journal of Geophysical Research: Solid Earth, 2020, 125, e2020JB020199.	3.4	17
108	Magmatic evolution of the Campi Flegrei and Procida volcanic fields, Italy, based on interpretation of data from well-constrained melt inclusions. Earth-Science Reviews, 2018, 185, 325-356.	9.1	16

#	Article	IF	CITATIONS
109	Oxygen isotope evidence for short-lived high-temperature fluid flow in the lower oceanic crust at fast-spreading ridges. Earth and Planetary Science Letters, 2007, 260, 524-536.	4.4	15
110	Sulfur Surprises in Deep Geological Fluids. Science, 2011, 331, 1018-1019.	12.6	15
111	Metamorphic replacement of mineral inclusions in detrital zircon from Jack Hills, Australia: Implications for the Hadean Earth: COMMENT. Geology, 2012, 40, e281-e281.	4.4	15
112	Blueschist-bearing metamorphic core complexes in the Qiangtang block reveal deep crustal structure of northern Tibet. Geology, 2000, 28, 19-22.	4.4	15
113	Petrology and geochemistry of the Kruuse Fjord Gabbro Complex, East Greenland. Geological Magazine, 1997, 134, 67-89.	1.5	14
114	The solubility of CePO4 monazite and YPO4 xenotime in KCl-H2O fluids at 800 °C and 1.0 GPa: Implications for REE transport in high-grade crustal fluids. American Mineralogist, 2017, 102, 2457-2466.	1.9	14
115	Metasomatic Phase Relations in the System CaO-MgO-SiO2-H2O-NaCl at High Temperatures and Pressures. International Geology Review, 2000, 42, 152-162.	2.1	13
116	Carbonate melts in the hydrous upper mantle. Contributions To Mineralogy and Petrology, 2020, 175, 1.	3.1	13
117	Deep Sourced Fluids for Peridotite Carbonation in the Shallow Mantle Wedge of a Fossil Subduction Zone: Sr and C Isotope Profiles of OmanDP Hole BT1B. Journal of Geophysical Research: Solid Earth, 2022, 127, .	3.4	11
118	Listvenite Formation During Mass Transfer into the Leading Edge of the Mantle Wedge: Initial Results from Oman Drilling Project Hole BT1B. Journal of Geophysical Research: Solid Earth, 2022, 127, .	3.4	11
119	Effect of Sediments on Aqueous Silica Transport in Subduction Zones. Geophysical Monograph Series, 2013, , 277-284.	0.1	7
120	Hydrothermal Alteration of the Ocean Crust and Patterns in Mineralization With Depth as Measured by Microâ€Imaging Infrared Spectroscopy. Journal of Geophysical Research: Solid Earth, 2021, 126, e2021JB021976.	3.4	7
121	Insights from X-ray absorption/fluorescence spectroscopy and ab-initio molecular dynamics on concentration and complexa-tion of Zr and Hf in aqueous fluids at high pressure and temperature. Journal of Physics: Conference Series, 2013, 430, 012122.	0.4	6
122	5. The Chemistry of Carbon in Aqueous Fluids at Crustal and Upper-Mantle Conditions: Experimental and Theoretical Constraints. , 2013, , 109-148.		6
123	The Influence of Pressure on the Properties and Origins of Hydrous Silicate Liquids in Earth's Interior. , 2018, , 83-113.		6
124	Spectroscopic and X-ray diffraction investigation of the behavior of hanksite and tychite at high pressures, and a model for the compressibility of sulfate minerals. American Mineralogist, 2013, 98, 1543-1549.	1.9	5
125	The Viscosity and Atomic Structure of Volatile-Bearing Melilititic Melts at High Pressure and Temperature and the Transport of Deep Carbon. Minerals (Basel, Switzerland), 2020, 10, 267.	2.0	5

126 Frontiers in geofluids: editorial. Geofluids, 2010, 10, 1-2.

0.7 4

#	Article	IF	CITATIONS
127	Deep water gives up another secret. Proceedings of the National Academy of Sciences of the United States of America, 2013, 110, 6616-6617.	7.1	2
128	Introduction to thematic issue on fluid and melt inclusions. Geofluids, 2013, 13, 395-397.	0.7	2
129	Presentation of the 2010 Roebling Medal of the Mineralogical Society of America to Robert C. Newton. American Mineralogist, 2011, 96, 948-949.	1.9	0